TISSUE ENGINEERING: Part A
Volume 17, Numbers 9 and 10, 2011

DOI: 10.1089/ten.tea.2010.0527

Lipolytic Function of Adipocyte/Endothelial Cocultures

Jennifer H. Choi, Ph.D.,[1] Evangelia Bellas, B.S.,[1] Jeffrey M. Gimble, M.D., Ph.D.,[2]
Gordana Vunjak-Novakovic, Ph.D.,[3] and David L. Kaplan, Ph.D.[1]

The rising incidence of adipose-related disorders such as obesity has prompted increased interest in the *in vitro* development of functional human soft tissues to study the disease and treatment options. Further, soft tissues maintained *in vitro* with a capacity to resemble *in vivo* tissues in structure and metabolic function would help gain insight into mechanisms involved in adipose tissue development. In the current study, the metabolic potential of adipose/endothelial cocultures on three-dimensional silk fibroin scaffolds was studied. Endothelial contributions to adipose lipogenesis and lipolysis were the focus of the study. Triglyceride accumulation, adipogenic gene transcript expression, and basal lipolysis measurements demonstrated the ability of this coculture system to retain metabolic levels obtained in adipocyte monocultures. Additionally, basal lipolysis was stimulated in mono- and coculture systems to a similar extent at 1.6- and 1.9-fold over controls, respectively. The ability to maintain adipose functions in these cocultures represents a step forward in the development of a tissue-engineered adipose tissue system exhibiting both endothelial lumens and metabolic functions.

Introduction

The development of a three-dimensional (3D) tissue-engineered adipose construct that structurally resembles native tissue and also exhibits metabolic function would serve as a significant step forward in the field of regenerative medicine. Current needs for *in vitro* models to better understand mechanisms of adipose tissue development and disease are increasing with the rise in incidence of obesity and adipose-related disorders.[1] While two-dimensional (2D) culture models of secretory systems, such as adipose tissue, contribute insight into adipose tissue biology, limitations rest in their ability to recapitulate biological effects of 3D tissue architecture and structure exhibited *in vivo*. Thus, the development of 3D adipose tissue models will provide physiologically relevant knowledge regarding human adipose biology.

Native adipose tissue comprises an extensive vasculature system[2] and is known to not only function as an energy storage depot, but also as a highly metabolic organ *in vivo*.[3] The ability of adipocytes to undergo both lipid accumulation and breakdown, or lipolysis, presents adipose tissue as an integral player in whole body homeostasis.[4] Specifically, adipocytes are composed of intracellular lipid or triglyceride (TG) stores that comprise roughly 95% of total adipocyte volume.[4] Adipogenesis is initiated and regulated through the activation of key transcription factors such as peroxisome proliferator-activated receptor gamma (*PPARγ*), and subsequent signaling cascades comprising members of the CCAAT/enhancer binding proteins family and Kruppel-like factor family, and various extracellular-mediated signaling pathways.[3] When other tissues are energy deprived, adipose tissue is signaled and lipolysis occurs, in which TGs are hydrolyzed to glycerol and fatty acids, one and three, respectively, per TG molecule.[5] In addition to responding to energy deprivation, adipose tissue also undergoes basal lipolytic activity, primarily mediated through adipose triglyceride lipase (*ATGL*) expression.[6]

Although many studies have explored various aspects of TG synthesis and lipolysis, to our knowledge, the metabolic function of adipocyte/endothelial cocultures in 3D remains less explored. The coculture of adipocytes with endothelial cells is an important strategy as it simulates the *in vivo* environment of adipose tissue through introduction of a vascular component. However, adipocyte/endothelial cocultures have been studied to a limited extent.[7,8] Recently, we conducted a study in which human adipose-derived mesenchymal stem cell (hASC)-differentiated adipocytes were cocultured with endothelial cells for 2 weeks *in vitro* to mimic more closely what is found *in vivo*. We found that in coculture, endothelial cells formed lumen-like structures, as evident through CD31 immunostaining, and that adipose tissue-like outcomes, such as lipid accumulation and leptin secretion, were evident.[8] In the numerous accounts of *in vitro* adipose tissue engineering approaches, including our previous study,[8] the focus has primarily been on 3D tissue

[1]Department of Biomedical Engineering, Tufts University, Medford, Massachusetts.
[2]Pennington Biomedical Research Center, Louisiana State University System, Baton Rouge, Louisiana.
[3]Department of Biomedical Engineering, Columbia University, New York, New York.

development through evidence of lipid accumulation. While adipose tissue engineering has progressed significantly in the recent years,[9] we are confident that a functional adipose tissue model in which lipogenesis and both basal and stimulated lipolysis are demonstrated will be a significant step forward for *in vitro* adipose tissue model needs.

In this study, we have utilized tissue engineering techniques to culture both adipogenic-differentiated hASCs and human umbilical vein endothelial cells (HUVECs) on 3D silk fibroin silk scaffolds. The use of hASCs for adipose tissue engineering is favorable as it is abundant and easily obtained through procedures such as liposuction and biopsies.[10] In addition, HUVECs are commercially available and have been utilized extensively as a lumen-forming human endothelial cell source.[11] Finally, we have previously demonstrated the ability of silk fibroin as a biomaterial substrate to support human adipogenesis both *in vivo* and *in vitro*,[8,12] thereby presenting itself as a favorable material for the development of a structurally and functionally relevant adipose tissue model. The goal of this study was to characterize this coculture system comprising hASCs and HUVECs on silk fibroin scaffolds with respect to key elements of lipogenesis and lipolysis. In addition, we were interested in exploring endothelial contributions to these two key metabolic processes to gain further insight into *in vivo* adipose tissue metabolic function. As endothelial cells are prevalent in native adipose tissue, we hypothesize that the presence of endothelial cells in our system will not inhibit levels of lipogenesis or lipolysis. Therefore, the development and characterization of an adipose tissue model demonstrating both structure and metabolic function similar to that of native tissue brings us a step forward in the development of a physiologically relevant adipose tissue model.

Materials and Methods

Materials

Cocoons from *Bombyx mori* silkworm were supplied by Tajimia Shoji Co. (Yokohama, Japan). hASCs were isolated according to published methods from subcutaneous adipose tissue donated with written consent by healthy (no evidence of diabetes or metabolic syndrome) volunteers undergoing elective liposurgery.[10] hASCs were isolated from the abdomen of a 44-year-old white woman (BMI 24.98). The work was reviewed and approved by the Pennington Biomedical Research Center Institutional Review Board. HUVEC and endothelial growth medium (EGM) were purchased from Lonza (East Rutherford, NJ); Dulbecco's modified Eagle's medium, Nutrient mix F-12 (1:1) containing L-glutamine (DMEM/F-12), fetal bovine serum (FBS), trypsin–EDTA, phosphate-buffered saline (PBS), human recombinant insulin, antibiotic–antimycotic (10,000 U/mL penicillin, 10,000 μg/mL streptomycin, and fungizone), trizol reagent, and Quant-iT PicoGreen dsDNA assay kit were purchased from Gibco–Invitrogen (Carlsbad, CA). Biotin, 2,4-Thiazolidinedione (TZD), dexamethasone, 3-isobutyl-1-methylxanthine (IBMX), pantothenate, Triglyceride assay kit, atrial neural peptide (ANP), isoproterenol (ISO), and propranolol (PRO) were purchased from Sigma-Aldrich (St. Louis, MO); proteinase-K was purchased from Fisher Scientific (Pittsburgh, PA); anti-Glut4 primary antibody was purchased from Applied Biosystems (Framingham, MA); universal staining kit was purchased from Vector Labs (Burlingame, CA); high-capacity cDNA reverse transcription kit, TaqMan® gene expression assays for glyceraldehydes-3-phosphate dehydrogenase (*GAPDH*) (Product # Hs99999905_m1), *PPARγ* (Product # Hs00234592_m1), glucose transporter 4 (*Glut4*) (Product # Hs00168966_m1), Leptin (Product # Hs00174877_m1), and *ATGL* (Product # Hs00386101_m1) were purchased from Applied Biosystems (Carlsbad, CA).

Preparation of aqueous silk scaffolds

Aqueous silk solution was prepared as previously described.[13] The resulting silk solution (7%–8% w/v) was further diluted to yield a 6% silk solution. Porous (500–600 μm pore size) aqueous silk scaffolds were prepared as previously described.[13] A biopsy punch was utilized to obtain final 4 × 2 mm (diameter × height) porous scaffolds.

Mono- and coculture on silk scaffolds

Isolated hASCs were cultured in DMEM/F-12 supplemented with 10% FBS and 1% antibiotic–antimycotic (ASC medium) and media were replenished every 3 days.[14] HUVECs were expanded in EGM and media were replenished every 2 days. At confluency, adipogenic differentiation was induced for 7 days in 2D (original seeding density 5000 cells/cm^2), in DMEM/F-12 medium containing 3% FBS, 1% penicillin–streptomycin, 33 μM biotin, 17 μM pantothenate, 1 μM insulin, 1 μM dexamethasone, 500 μM IBMX, and 5 μM TZD. The adipocyte maintenance medium was composed of differentiation medium minus IBMX and TZD.

HUVECs (Passage 4) were seeded on silk scaffolds (500,000 cells/scaffold) and cultured for 7 days. Seven-day adipogenic differentiated hASCs (note: in this article, we refer to these cells as differentiated adipocytes) (235,000 cells/scaffold) or undifferentiated hASCs (235,000 cells/scaffold) were then added to HUVEC-seeded scaffolds for coculture. Undifferentiated hASCs were expanded in culture throughout duration of adipogenic differentiation such that passage number for hASCs and adipocytes were consistent (passage 4 ASCs/adipocytes were utilized for this study). Coculture scaffolds consisted of either differentiated adipocytes with HUVECs or undifferentiated hASCs with HUVECs, and were cultured in 1:1 EGM:maintenance medium and 1:1 EGM:ASC, respectively, for 14 days, with medium replacement every 2 days. Scaffolds consisting of undifferentiated hASC monocultures, differentiated adipocyte monocultures, or HUVEC monocultures were used as controls.

DNA assay

Scaffolds were harvested in TEX (10 mM Tris, 1 mM EDTA, and 1% triton X-100) and Proteinase K, and stored at −20°C. Samples were thawed, and incubated in 56°C water bath overnight for complete sample digestion. Samples were then chopped (or minced into small pieces with sterile surgical scissors) and centrifuged at 15,700 *g* for 10 min, 4°C, and supernatants collected. DNA content was determined fluorometrically at 480/525 nm (ex/em) using an FLx800 spectrofluorometer (BioTek, Winooski, VT). The amount of DNA was determined by interpolation from a standard

curve prepared using λDNA in 10 mM Tris-HCl (pH 7.4), 5 mM NaCl, and 0.1 mM EDTA over a range of concentrations, according to manufacture protocols.

Lipid accumulation

Scaffolds were harvested in sodium dodecyl sulfate buffer (0.1% w/v) and stored at −20°C. Upon thawing, scaffolds were minced into small pieces and sonicated briefly, and centrifuged at 15,700 *g* for 10 min at 4°C, and supernatants were collected. TG was measured using an enzymatic assay, in which a quinoneimine dye is produced proportional to glycerol, and quantified at 540 nm. Additionally, scaffolds were fixed in 2M sucrose overnight for histology. Scaffolds were embedded in OCT medium, and frozen scaffolds were sectioned (10 μm sections) and stained with Oil Red O (ORO).

Glut4 immunohistochemistry

Scaffolds were fixed in 10% formalin at 4°C for up to 3 weeks before automated paraffin processing and embedding.[8] Paraffin blocks were sectioned (5 μm sections) and on the first day, sections underwent xylene washes, dehydration, and microwave pretreatment in 0.01 M citric acid buffer (pH 6). Endogenous peroxidase activity was quenched in 3% hydrogen peroxide in methanol. Blocking of unspecified sites was performed with normal horse serum, followed by incubation in 1:150 dilution of primary anti-human Glut4 antibody in PBS overnight. Sections were incubated with biotinylated universal secondary antibody for 1 h, incubated 30 min in Vectastain ABC reagent, and developed with 3,3′-diaminobenzidine/hydrogen peroxide for 10 min. Sections were counterstained with hematoxylin and mounted according to standard protocols.

Free glycerol detection

Medium samples were collected and stored at −80°C. Samples were thawed, and centrifuged at 15,700 *g* for 10 min at 4°C, and supernatants collected. Detected glycerol was measured (540 nm) using the TG kit described earlier, however, excluding the hydrolysis step. Glycerol levels detected in medium samples from blank scaffolds were subtracted from all medium samples.

Real-time RT-PCR

Total RNA was extracted from cells using Trizol reagent. Scaffolds harvested in Trizol were stored at −80°C. After thawing, scaffolds were chopped and centrifuged at 15,700 *g* for 10 min at 4°C. Supernatants were transferred to new tubes and RNA isolated according to supplier's instructions. Reverse transcription was performed using high-capacity cDNA reverse transcription kit following supplier's instructions. Commercially available primers and probes from TaqMan® Gene Expression Assays were utilized for target genes *PPARγ*, Leptin, and *ATGL*, and normalized to the housekeeping gene, *GAPDH*, using the 2ΔΔCt formula. Specifically, real-time RT-PCR reactions were performed using an ABI 7500 Sequence Detection System (Applied Biosystems) at 50°C for 2 min, 95°C for 10 min, followed by 40 cycles of amplifications, consisting of a denaturation step at 95°C for 15 s, and extension step at 60°C for 1 min.

Stimulating/inhibiting lipolysis

Lipolysis was stimulated with 1 μM ANP or 1 μM ISO and inhibited with 100 μM PRO in 2D adipogenic differentiated hASC cultures. Cells were washed with serum-free DMEM/F-12, and incubated in DMEM/F-12 with 0.1% BSA overnight. The following day, cultures were incubated in DMEM/F-12 with 3% BSA containing ANP, ISO, PRO, or PBS (control) for 3 h. Supernatants were collected, and stored at −20°C. Supernatants were thawed, and evaluated for glycerol content according to protocol described above. Following the same protocol, 3D differentiated cultures (mono- and cocultures) were stimulated (ISO only) and inhibited (PRO), and secreted glycerol content measured.

Statistical analysis

All reported values were averaged ($n = 3$) and expressed as mean ± standard deviation. Statistical differences were determined by Student's two-tailed *t*-test and differences were considered statistically significant at $p < 0.05$.

Results

Lipogenesis

Cell seeding and proliferation. All scaffolds were evaluated for their DNA content, as a measure of proliferation, at days 2, 6, and 14 from the start of coculture (Fig. 1A). At each time point, there were no significant differences in DNA content between mono- and cocultures; however, all groups had demonstrated an increase in DNA content from day 2 to 14 ($p < 0.05$). Endothelial monocultures contained very low initial DNA levels at days 2 and 6, but then proliferated to a great extent by day 14.

Lipid accumulation. All scaffolds were investigated for lipid content through TG quantification at days 2, 6, and 14 (Fig. 1B) and ORO staining (Fig. 1C, D, G, H). At day 2, while differentiated cultures exhibited greater TG levels compared with undifferentiated and endothelial cultures, there were no significant differences observed. By day 6, differentiated mono- and cocultures exhibited greater accumulated TG from undifferentiated and endothelial monocultures ($p < 0.05$); however, TG levels between differentiated mono- and cocultures were comparable. At day 14 culture, differentiated cultures retained TG levels, and remained significantly greater than undifferentiated and endothelial cultures. However, undifferentiated mono- and cocultures increased in TG content from day 6 levels ($p < 0.05$). Similar to days 2 and 6, no differences were noted between mono- and cocultures. Positive ORO was exhibited in all differentiated cultures, whereas undifferentiated cultures (insets) contained considerably lower levels of staining.

Glut4 immunohistochemistry. At day 14, Glut4 was stained within each group (Fig. 1E, F, I, J). Differentiated mono- and cocultures exhibited a significant positive stain compared with undifferentiated cultures (insets). Higher magnification images (Fig. 1F, J) show darker stain in the cell cytoplasm and membrane compared with undifferentiated controls, demonstrating increased Glut4 content and membrane recruitment. Although positive staining is evident in

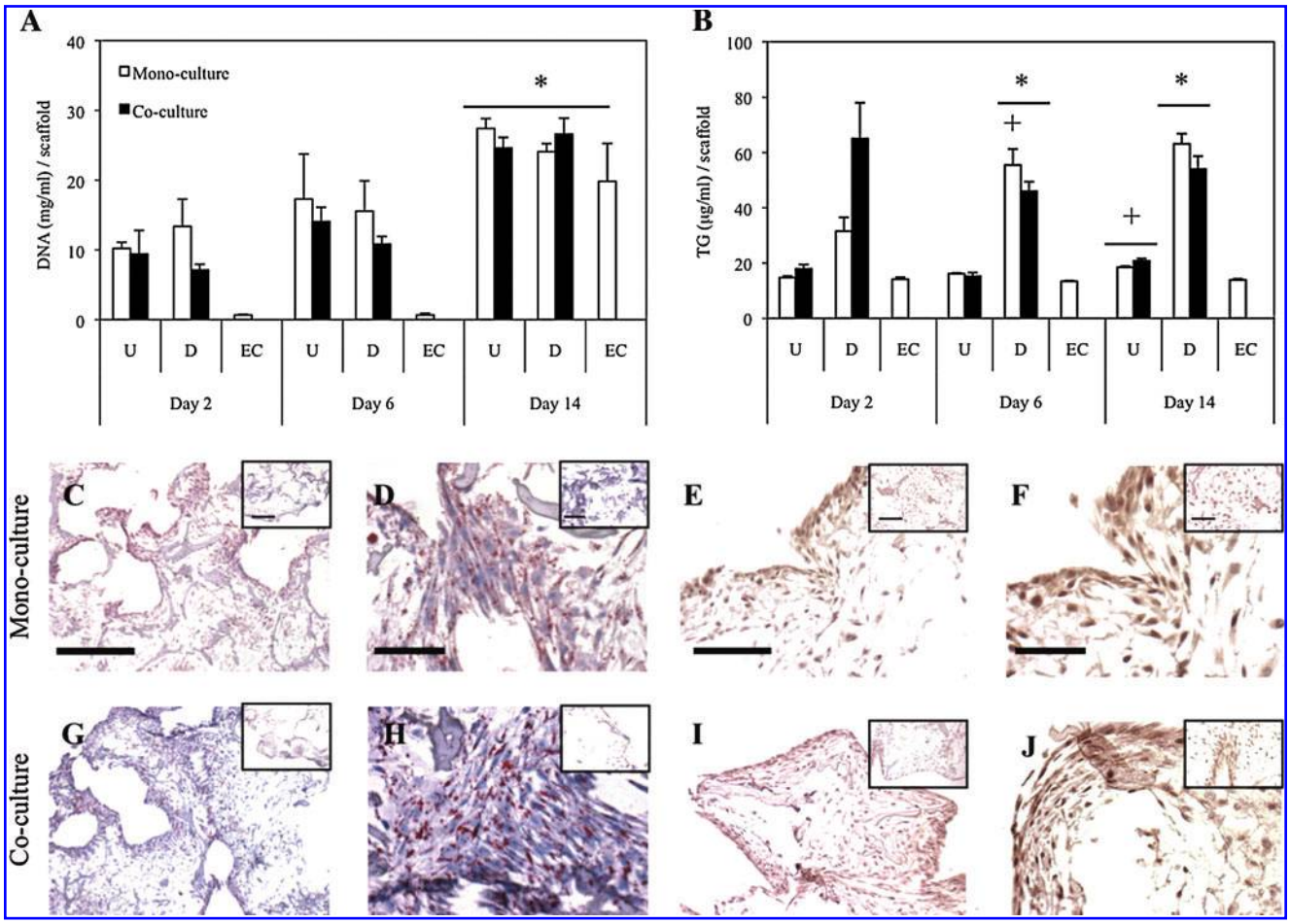

FIG. 1. Lipogenic activity of undifferentiated hASC mono-/cocultures (U), adipogenic differentiated mono-/cocultures (D), and endothelial monocultures (EC) were evaluated. **(A)** DNA content was determined at days 2, 6, and 14 of culture. All cultures proliferated to significant extent by day 14 ($^*p < 0.05$). Lipid was quantified **(B)** and day 14 Oil Red O stained positive in all differentiated cultures **(C, D, G, H)** compared to undifferentiated cultures (insets). Differentiated cultures accumulated more lipid than undifferentiated and endothelial cultures ($^*p < 0.05$). Day 6 differentiated monocultures and day 14 undifferentiated cultures also showed increases from previous time points ($^+p < 0.05$). Glut4 was positively stained in differentiated cultures via immunohistochemistry **(E, F, I, J)** compared to undifferentiated cultures (insets). Scale bars: **(C, E, G, I)** 500 μm (original magnification 4×); **(D, F, H, J)** 100 μm (original magnification 20×). hASC, human adipose-derived mesenchymal stem cell; Glut4, glucose transporter 4. Color images available online at www.liebertonline.com/tea

both mono- and cocultures, a quantitative difference between mono- and cocultures of Glut4 protein expression was not concluded.

Lipolysis: Free glycerol secretion

The degree of basal lipolysis that was occurring in all scaffolds was measured via free glycerol release into supernatants (Fig. 2). At each time point, differentiated mono- and cocultures secreted significantly greater glycerol compared with undifferentiated mono-/coculture and endothelial cultures ($p < 0.05$). There were no significant differences noted between mono- and cocultures for all groups, similar to TG levels. Glycerol secretion levels fluctuated over time, but no significant differences were observed, demonstrating basal glycerol secretion in differentiated cultures.

Transcript expression

Expression of key adipogenic mRNA transcripts was evaluated via real-time RT-PCR analyses (Fig. 3). *PPARγ* gene expression was evident in all cultures; however, there were no significant differences between undifferentiated (mono/co) and differentiated (mono/co) cultures (Fig. 3A). Endothelial monocultures exhibited basal levels of *PPARγ*, in which expression levels were significantly less than all other cultures. *Glut4* expression demonstrated increased levels in differentiated cultures compared with undifferentiated (though not significant), and similar to *PPARγ*, there were no significant differences between mono- and cocultures at each time point (Fig. 3B). Leptin transcript levels were significantly greater in differentiated cultures than in undifferentiated cultures, and additionally, differentiated cocultures retained similar levels throughout the culture, whereas differentiated monocultures increased in leptin expression with time (Fig. 3C). Finally, the key lipolysis enzyme, *ATGL*, was evaluated (Fig. 3D). Similar to other transcripts, there were no differences noted between mono- and cocultures. At day 2 and 6, *ATGL* expression levels for the undifferentiated (mono/co) and differentiated (mono/co) cultures were similar, whereas endothelial monocultures exhibited significantly greater levels at all time points. By day

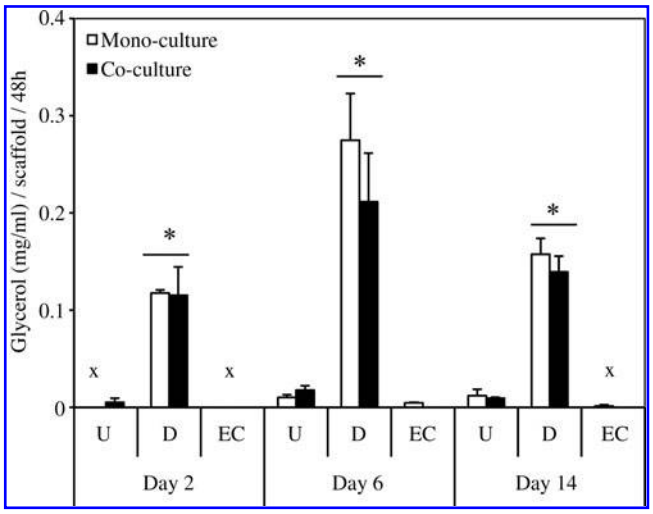

FIG. 2. Lipolytic activity of undifferentiated hASC mono-/cocultures (U), adipogenic differentiated mono-/cocultures (D), and endothelial monocultures (EC) were evaluated by measuring basal glycerol levels after 2, 6, and 14 days of culture. Differentiated mono-/cocultures secreted greater glycerol than undifferentiated cultures and endothelial monocultures (*$p < 0.05$). No significant differences between mono- and cocultures in glycerol secretion. Undetectable levels indicated by (x).

14, differentiated (mono/co) cultures had decreased *ATGL* expression significantly from day 6, demonstrating less basal lipolysis.

Stimulating/inhibiting lipolysis

The ability to stimulate and inhibit lipolysis was first demonstrated in adipogenic differentiated hASC 2D cultures (Fig. 4A). Both ANP and ISO stimulated significantly greater glycerol release relative to control conditions ($p < 0.05$). ANP-stimulated cultures yielded roughly threefold increase in glycerol over control cultures, whereas ISO yielded a fourfold increase in glycerol secretion. PRO, however, did not decrease glycerol release significantly compared with control cultures. Following 2D studies, similar protocols were implemented to both adipogenic mono- and cocultures in 3D (Fig. 4B). However, only ISO was utilized to stimulate 3D cultures, as this yielded a greater fold increase in 2D studies compared with ANP. ISO stimulated 3D adipogenic monocultures and cocultures 1.6 and 1.9 times that of controls, respectively. PRO inhibited adipogenic monocultures by 40% as compared with controls, but did not inhibit glycerol levels of cocultures. Despite this discrepancy, there were no significant differences noted between mono- and cocultures.

Discussion

The development of an *in vitro* adipose tissue model that resembles *in vivo* tissue would serve as a significant step forward in the study of adipocyte biology. Further, the increasing incidence of obesity and adipose-related disease adds to the increased need to understand mechanisms of disease onset and progression. In this study, we were interested in further developing an *in vitro* adipose tissue model using tissue engineering strategies. Previously, we demonstrated the ability to coculture hASCs with HUVECs in 3D silk fibroin scaffolds.[8] As a follow-up, we performed the present study to further investigate the metabolic activity of these tissue-engineered constructs, in addition to exploring endothelial contributions to the engineered adipose tissue. Specifically, we were interested in observing how the presence of endothelial cells affected the ability of adipocytes to accumulate lipid and undergo lipolysis. Additionally, we included mono- and cocultures of endothelial cells with undifferentiated hASCs, serving as an internal control for adipogenic differentiation. We found that cocultured endothelial cells contributed to structural organization, as shown through our previous work,[8] and, in this study, that the presence of endothelial cells in coculture retained metabolic activity exhibited in differentiated adipocyte monocultures.

We demonstrated in both qualitative and quantitative methods that TG synthesis was not affected by the presence of endothelial cells. Total DNA content of both mono- and cocultures within the silk scaffolds was measured, and all groups showed peak levels at day 14 (Fig. 1A). Previous studies indicated a lag in HUVEC proliferation after attachment to silk scaffolds,[8] and similarly, we see this behavior in the current study. We show increased TG in differentiated cultures relative to undifferentiated cultures, and similar levels between differentiated mono- and cocultures (Fig. 1B). Additionally, we show ORO-positive adipocytes clustered throughout scaffolds consisting of multiple lipid droplets per adipocyte (Fig. 1C, D, G, H). *Glut4*, a well-known marker of adipogenic differentiation, acts as a key mediator of glucose homeostasis, and plays an active role in TG synthesis.[12,15,16] We investigated *Glut4* at the transcript (Fig. 3B) and protein expression level (Fig. 1E, F, I, J). We observed, at day 6, *Glut4* transcript level expression peaks, and at day 14, protein expression is evident. However, we do not observe a difference between differentiated mono- and cocultures. *PPARγ* transcript levels show a peak in differentiated cultures at day 6; however, a significant difference between mono- and cocultures was not observed (Fig. 3A). The lack of clear trends in expression of *PPARγ* may be because it is an early marker necessary for adipogenic induction.[3] As adipogenesis was induced in 2D before seeding onto silk scaffolds, *PPARγ* expression most likely peaked before seeding. Finally, leptin transcript levels were assessed as a means to deduce how mature the adipocytes were, as leptin is a mature adipokine secreted by adipocytes (Fig. 3C).[17] We see significant expression of differentiated cultures at each time point relative to undifferentiated cultures, though overall expression remained relatively stable throughout culture. We previously reported that leptin secretion increases with time[8]; however, the current study may indicate that in both mono- and cocultures, as the adipocytes mature, leptin signaling is affected at the post-transcriptional level.

Basal lipolysis measurements indicate a significant increase in glycerol release in differentiated cultures compared with undifferentiated and endothelial cultures, which correlates to TG content (Fig. 2). We do not see any differences between adipocyte mono- and cocultures, which also coincides with what we find in TG synthesis analyses. In addition, *ATGL* transcript expression was assessed (Fig. 3D). Interestingly, while we do not see any differences in transcript expression of undifferentiated and differentiated cultures, endothelial monocultures exhibited high expression

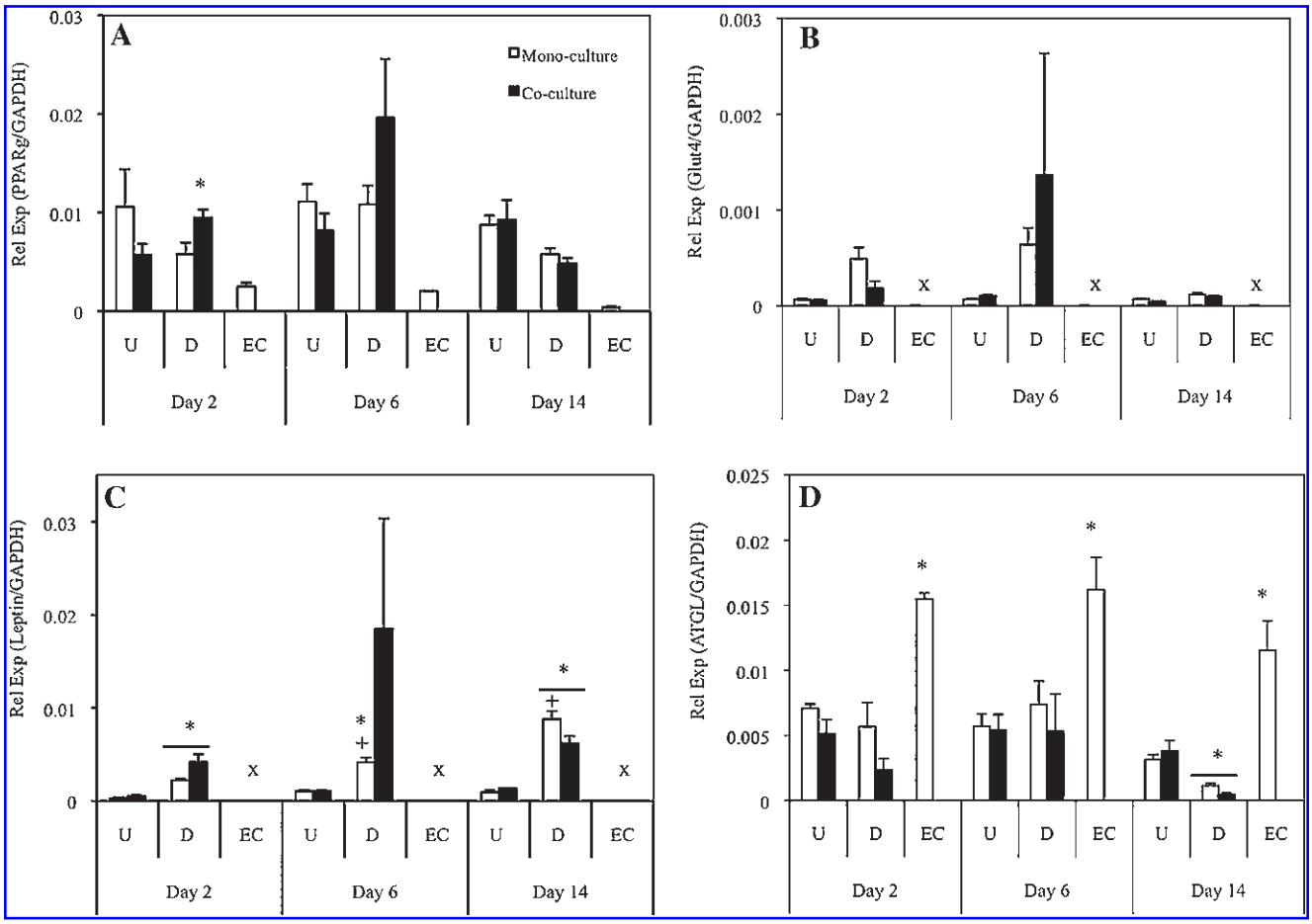

FIG. 3. Adipogenic gene expression on days 2, 6, and 14 of culture. *PPARγ* **(A)**, *Glut4* **(B)**, leptin **(C)**, and *ATGL* **(D)** expression was measured. Differences were exhibited between adipogenic differentiated and undifferentiated cultures in *PPARγ* and leptin expression ($^*p < 0.05$). Differentiated monocultures show increased leptin expression at days 6 and 14 from previous time points ($^+p < 0.05$). Endothelial monocultures show increased *ATGL* expression at all time points compared with both undifferentiated and differentiated cultures; differentiated mono- and cocultures exhibited significantly less *ATGL* expression compared with undifferentiated cultures at day 14 ($^*p < 0.05$). Undetectable levels indicated by (x). *PPARγ*, proliferator-activated receptor gamma; *ATGL*, adipose triglyceride lipase.

levels throughout the culture. A previous study in which Jin and colleagues exposed HUVECs to varying concentrations of IL-1β or TNF-α, reported that an endothelial lipase was expressed at the mRNA level and found to be secreted after 24h exposure.[18] Further studies therefore need to be performed to provide additional explanation regarding endothelial expression of *ATGL*. *ATGL* has been shown to be expressed in both murine and human adipocytes; however, there are conflicting reports as to its role in basal lipolysis.[6,19,20] To our knowledge, *ATGL* expression has not been evaluated specifically in adipogenic-differentiated hASCs; therefore, though we see that *ATGL* transcript expression trends do not correlate directly to glycerol release, further studies need to be performed to measure *ATGL* protein content.

Finally, we measured adipose tissue function through stimulating or inhibiting lipolysis. Previously, studies have reported the ability to stimulate and inhibit lipolysis of 3D tissue-engineered adipose constructs, and thus we were interested in demonstrating this in both our mono- and coculture system.[21] Adipocyte adrenergic receptors are partly responsible for regulating the lipolysis pathway, and thus we utilized commercial β-adrenergic stimulators and inhibitors.[22] Preliminary 2D screens demonstrated functionality of β-receptor stimulants and inhibitors, and since ISO stimulated glycerol to a greater degree than ANP, we chose to use ISO for 3D studies. PRO did not significantly decrease glycerol secretion and maintained the same level as control (PBS) cultures in both 2D and 3D. In summary, we observed that both mono- and cocultures respond to lipolysis stimulants and inhibitors to a similar degree.

To our knowledge, there are no reports of how adipocyte/endothelial coculture may affect metabolic activity of *in vitro* adipose tissue. The lack of an effect that endothelial cells had on TG synthesis, lipolysis, and lipolytic control demonstrates that in this system, HUVECs act as a structural component forming endothelial-like lumens in coculture,[8] while also retaining adipose tissue metabolic function, as exhibited by adipocytes alone. We recognize that the current reported outcomes are based on a single hASC donor, and thus a follow-up donor comparison study to investigate donor-to-donor differences was conducted with four donors on 3D aqueous silk scaffolds (Supplementary Fig. S1; Supplementary Data are available online at www.liebertonline.com/tea).

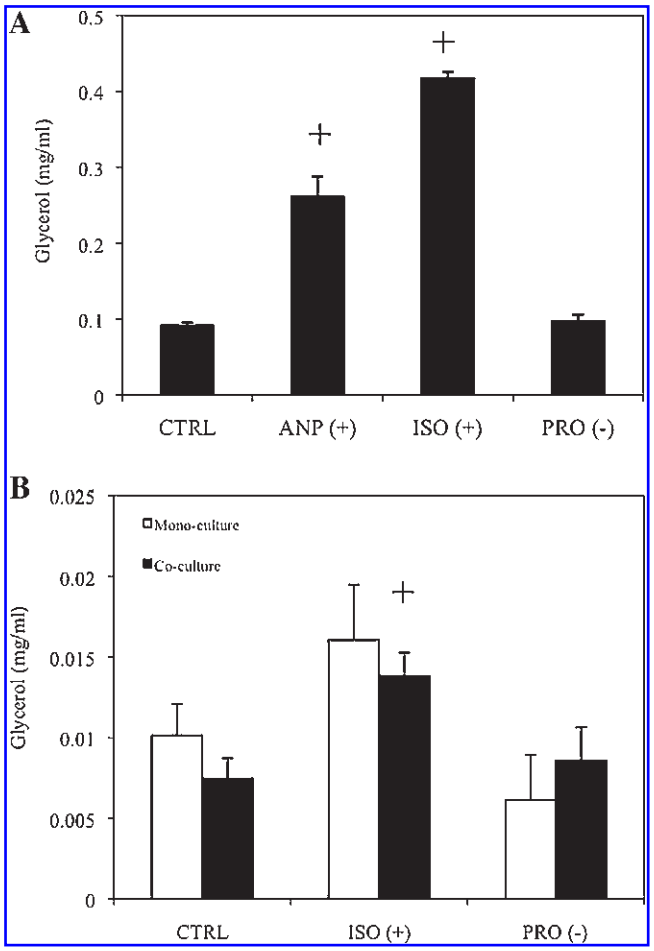

FIG. 4. Stimulating and inhibiting basal lipolysis at day 14 culture. hASCs were differentiated in two-dimensional, and lipolysis was stimulated with atrial neural peptide (ANP) or isoproterenol (ISO) or inhibited with propranolol (PRO), and free glycerol measured **(A)**. Both ANP and ISO stimulated increased glycerol release compared with phosphate-buffered saline control ($^{+}p < 0.05$). Subsequently, adipogenic differentiated mono-/cocultures in three-dimensional were stimulated or inhibited, and glycerol content measured **(B)**. ISO stimulated increased glycerol in coculture compared with coculture control ($^{+}p < 0.05$).

We did not exhibit significant differences between donors regarding hASC proliferation, hASC differentiated adipocyte TG accumulation, and glycerol secretion, suggesting that our data are representative of the general hASC population. Future work including cocultures of hASCs from multiple donors, however, would provide additional validation.

The contribution of endothelial cells to our coculture system may include the facilitation of necessary signals/transport to help maintain active adipose tissue in the 3D system. Additional studies to quantify individual cell types within the coculture system would provide insight regarding endothelial contributions in our system. This may include transduction with tracking dyes for additional observation, or flow cytometry studies to characterize each cell type in coculture. This study, however, further enhances the potential of our strategy for adipose tissue engineering to be used as an *in vitro* 3D adipose tissue model. Ongoing studies include long-term coculture, and future studies will need to be conducted to further understand the complexity of this coculture relationship at both functional and mechanistic levels.

Acknowledgments

The authors would like to thank Ning Lai for providing support for the TG quantification assay, and Sorabh Kothari and Tina Jumani for help in silk scaffold production. We also thank the NIH P41 Tissue Engineering Resource Center (P41 EB002520) and AFIRM for support of aspects of research on soft tissue engineering.

Disclosure Statement

The authors declared no conflicts of interest.

References

1. Korner, J., Woods, S.C., and Woodworth, K.A. Regulation of energy homeostasis and health consequences in obesity. Am J Med **122,** S12, 2009.
2. Hausman, G.J., and Richardson, R.L. Adipose tissue angiogenesis. J Anim Sci **82,** 925, 2004.
3. Rosen, E.D., and MacDougald, O.A. Adipocyte differentiation from the inside out. Nat Rev Mol Cell Biol **7,** 885, 2006.
4. Arner, P. Human fat cell lipolysis: biochemistry, regulation and clinical role. Best Pract Res Clin Endocrinol Metab **19,** 471, 2005.
5. Lafontan, M., and Langin, D. Lipolysis and lipid mobilization in human adipose tissue. Prog Lipid Res **48,** 275, 2009.
6. Miyoshi, H., Perfield, J.W., 2nd, Obin, M.S., and Greenberg, A.S. Adipose triglyceride lipase regulates basal lipolysis and lipid droplet size in adipocytes. J Cell Biochem **105,** 1430, 2008.
7. Lai, N., Jayaraman, A., and Lee, K. Enhanced proliferation of human umbilical vein endothelial cells and differentiation of 3T3-L1 adipocytes in coculture. Tissue Eng Part A **15,** 1053, 2008.
8. Kang, J.H., Gimble, J.M., and Kaplan, D.L. *In vitro* 3D model for human vascularized adipose tissue. Tissue Eng Part A **15,** 2227, 2009.
9. Gomillion, C.T., and Burg, K.J. Stem cells and adipose tissue engineering. Biomaterials **27,** 6052, 2006.
10. Dubois, S.G., Floyd, E.Z., Zvonic, S., *et al.* Isolation of human adipose-derived stem cells from biopsies and liposuction specimens. Methods Mol Biol **449,** 69, 2008.
11. Frerich, B., Zuckmantel, K., Winter, K., Muller-Durwald, S., and Hemprich, A. Maturation of capillary-like structures in a tube-like construct in perfusion and rotation culture. Int J Oral Maxillofac Surg **37,** 459, 2008.
12. Mauney, J.R., Nguyen, T., Gillen, K., Kirker-Head, C., Gimble, J.M., and Kaplan, D.L. Engineering adipose-like tissue *in vitro* and *in vivo* utilizing human bone marrow and adipose-derived mesenchymal stem cells with silk fibroin 3D scaffolds. Biomaterials **28,** 5280, 2007.
13. Kim, U.-J., Park, J., Kim, H.J., Wada, M., and Kaplan, D.L. Three-dimensional aqueous derived biomaterial scaffolds from silk fibroin. Biomaterials **26,** 2775, 2005.
14. McIntosh, K., Zvonic, S., Garrett, S., *et al.* The immunogenicity of human adipose-derived cells: temporal changes *in vitro*. Stem Cells **24,** 1246, 2006.
15. Hauner, H., Rohrig, K., Spelleken, M., Liu, L.S., and Eckel, J. Development of insulin-responsive glucose uptake

and GLUT4 expression in differentiating human adipocyte precursor cells. Int J Obes Relat Metab Disord **22,** 448, 1998.
16. Hou, J.C., and Pessin, J.E. Ins (endocytosis) and outs (exocytosis) of GLUT4 trafficking. Curr Opin Cell Biol **19,** 466, 2007.
17. Yang, R., and Barouch, L.A. Leptin signaling and obesity: cardiovascular consequences. Circ Res **101,** 545, 2007.
18. Jin, W., Sun, G.S., Marchadier, D., Octtaviani, E., Glick, J.M., and Rader, D.J. Endothelial cells secrete triglyceride lipase and phospholipase activities in response to cytokines as a result of endothelial lipase. Circ Res **92,** 644, 2003.
19. Bezaire, V., Mairal, A., Ribet, C., *et al.* Contribution of adipose triglyceride lipase and hormone-sensitive lipase to lipolysis in hMADS adipocytes. J Biol Chem **284,** 18282, 2009.
20. Ryden, M., Jocken, J., van Harmelen, V., *et al.* Comparative studies of the role of hormone-sensitive lipase and adipose triglyceride lipase in human fat cell lipolysis. Am J Physiol Endocrinol Metab **292,** E1847, 2007.
21. Fischbach, C., Seufert, J., Staiger, H., *et al.* Three-dimensional *in vitro* model of adipogenesis: comparison of culture conditions. Tissue Eng **10,** 215, 2004.
22. Lafontan, M., and Berlan, M. Fat cell adrenergic receptors and the control of white and brown fat cell function. J Lipid Res **34,** 1057, 1993.

Address correspondence to:
David L. Kaplan, Ph.D.
Department of Biomedical Engineering
Tufts University
4 Colby St.
Medford, MA 02155

E-mail: david.kaplan@tufts.edu

Received: September 5, 2010
Accepted: January 18, 2011
Online Publication Date: March 1, 2011

This article has been cited by:

1. Rui Yao, Yanan Du, Renji Zhang, Feng Lin, Jie Luan. 2013. A biomimetic physiological model for human adipose tissue by adipocytes and endothelial cell cocultures with spatially controlled distribution. *Biomedical Materials* **8**:4, 045005. [CrossRef]
2. Jeffrey Gimble, Maryam Rezai Rad, Shaomian YaoAdipose Tissue-Derived Stem Cells and Their Regeneration Potential 241-258. [CrossRef]
3. Elizabeth McRae, Jaime Boris. 2013. Independent evaluation of low-level laser therapy at 635 nm for non-invasive body contouring of the waist, hips, and thighs. *Lasers in Surgery and Medicine* **45**:1, 1-7. [CrossRef]
4. Evangelia Bellas, Miri Seiberg, Jonathan Garlick, David L. Kaplan. 2012. In vitro 3D Full-Thickness Skin-Equivalent Tissue Model Using Silk and Collagen Biomaterials. *Macromolecular Bioscience* **12**:12, 1627-1636. [CrossRef]